Kirkendall Voids in the Intermetallic Layers of Solder Joints in MEMS

Kerstin Weinberg *, Thomas Böhme and Wolfgang H. Müller

Institut für Mechanik, Lehrstuhl für Kontinuumsmechanik und Materialtheorie (LKM), Sekr. MS-2, Technische Universität Berlin, Einsteinufer, 10587 Berlin, Germany

Abstract

Microelectronic systems consist of the functional chip unit itself and a surrounding package which includes several electro-mechanical connections, e.g., solder joints between different metal layers. Experimental observation shows that aging of the solder alloy as well as the formation and growth of so-called KIRKENDALL voids significantly contributes to the degradation of the joining capability.

Starting with a phenomenological explanation of the KIRKENDALL effect we present in this contribution a constitutive model for void nucleation and growth. The model accounts for the effects of vacancy diffusion, surface tension and rate-dependent plastic deformation on ensembles of spherical voids. It can be applied to predict the temporal development of voids in solder joints. Numerical simulations on the material point level provide inside into the (not yet completely understood) mechanisms of failure by formation and growth of KIRKENDALL voids and show the potential of the model for the failure analysis of joints.

Key words: KIRKENDALL effect; Intermetallic compounds; Nucleation; Vacancy diffusion; Plastic deformation
PACS: 61.72.Qq; 61.72.jd; 68.35.Fx; 66.30.-h; 62.20.F-

1. Introduction

The functional unit of Micro-Electro-Mechanical-Systems (MEMS) is typically a Si-chip, however, different metallic joints are required to provide electrical and mechanical connections. If such connections, *e.g.*, solder joints and plated through holes, fail this will typically cause failure of the whole MEM. The setup is illustrated exemplarily in Figure 1 for a Flip Chip packaging. Solder balls as well as small joints, which are typically made of Sn-containing alloys (*e.g.*, Sn-Ag or Sn-Ag-Cu), hold the multi-layered unit in position and provide electrical conductivity between the coppered layers. "Aging" of the solder alloy, such as phase separation, coarsening and the growth of InterMetallic Compounds (IMCs), as well as the formation and growth of pores and cracks significantly effects the life expectation of the joints and considerably influences the reliability of the MEMS.

Initial IMCs develop due to interfacial reactions when, during manufacturing, the (molten) Sn-rich solder wets the copper pad. In particular, Cu_3Sn and Cu_6Sn_5 will form to irregular shaped layers of initially 2-5 μm height together with further intermetallics. As a consequence of thermal and mechanical loading during service the IMCs grow and may reach a thickness of 20 μm and more. Additionally, KIRKENDALL voids nucleate and grow (mainly) within the IMCs. The KIRKENDALL effect can be described as follows: neighboring phases or compounds change in a way that the volume of one region grows and the volume of the another phase reduces. In

* corresponding author: Tel.: +49-30-314-24214; fax: +49-30-314-24499

Email addresses: kerstin.weinberg@tu-berlin.de (Kerstin Weinberg), thomas.boehme@tu-berlin.de (Thomas Böhme), wolfgang.h.mueller@tu-berlin.de (Wolfgang H. Müller).

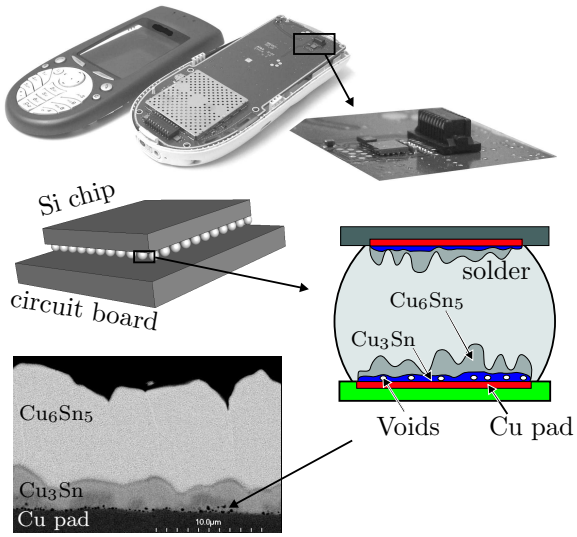

Fig. 1. Voids in intermetallic compounds at copper-solder interfaces in MEMS (micrograph from [8]).

case of Sn-based solders such regions are typically the IMCs Cu_3Sn and Cu_6Sn_5 from where the diffusion of Cu into the Sn-rich solder is much *faster* than the inverse diffusion of Sn. Because of the unbalanced Cu-Sn diffusion vacancies are left behind which coalesce to form KIRKENDALL voids. Additional vacancies and defects in the crystal lattices are generated by plastic deformation of the solder material and assist in the process of void growth and material degradation.

2. Model of void nucleation and growth

To model void condensation out of the scale of crystal lattice defects as a void-nucleating mechanism we idealize the material as a homogenous medium with arbitrarily distributed vacancies and employ a model of *vacancy condensation*.

Let us consider a small void possibly just a few atomic spacings in diameter surrounded by a supersaturated background vacancy concentration c_b. We assume a steady state vacancy concentration profile, *i.e.*, $\partial c_{\rm vac}/\partial t \ll \partial J/\partial x$, where c is the vacancy fraction and $J_{\rm vac}$ is the vacancy flux. With b being the (large) radius of the basin of attraction around the void with characteristic radius a, *cf.*, Figure 2, and $b/a \to \infty$, the diffusion equation simplifies to:

$$\frac{\partial}{\partial r}\left(r^2\frac{\partial c}{\partial r}\right) = 0\,, \tag{1}$$

with boundary conditions $c(r=a)=c_a$ and $c(r=b)=c_b$. The equilibrium vacancy concentration near a free surface is given by

$$c_0 = e^{-E_V/kT} \tag{2}$$

and the concentration c_a at the void surface follows from the GIBBS-THOMSON effect as

$$c_a = c_0 e^{d/a} \quad \text{with} \quad d = \frac{2\gamma V_V}{kT}\,. \tag{3}$$

In these expressions γ is the surface tension, V_V the atomic volume, k the BOLTZMANN constant and E_V is the free-energy gain/loss resulting from adding a vacancy into the system. The solution of (1)-(3) is elementary, namely

$$c(r) = c_b - (c_b - c_a)\frac{a}{r}\,. \tag{4}$$

For void growth to take place there must be a net flux of vacancies *into* the void, which requires $c_b > c_a$. For very small values of a_0 or c_b this inequality is not satisfied and voids fail to grow. The value of radius a_0 in expression (3) which equals a given value of c_b marks the inception of void growth, *i.e.*, a *critical nucleation size*.

The vacancy flux J is defined to be the change of volume per unit area and time, *viz.*

$$J(r) = -\frac{1}{4\pi a^2}\frac{\mathrm{d}}{\mathrm{d}t}\left(\frac{4}{3}\pi a^3\right) = -\dot{a}(r)\,. \tag{5}$$

Applying FICK's law $J(r) = -D_V\frac{\partial c}{\partial r}$ to Eq. (5) yields for voids of radius a by means of Eq. (4):

$$\dot{a}(a) = \frac{D_V}{a}\left(c_b - c_0 e^{d/a}\right)\,, \tag{6}$$

where D_V is the vacancy diffusion coefficient, more precisely, the tracer diffusion coefficient of vacancies, *cf.*, [5].

The background vacancy concentration c_b can be subjected to a "void volume balance" of the form:

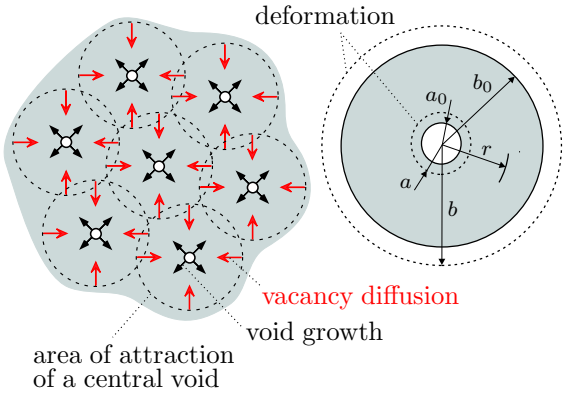

Fig. 2. Model of vacancy diffusion and model of a single void before and after deformation.

$$\dot{c}(t) = s(t) - \int_{a_{\text{vac}}}^{a_{\max}} \tilde{d}(a,t)\,\dot{a}(a)\,4\pi a^2\,\mathrm{d}a$$
$$= s(t) - \int_{a_{\text{vac}}}^{a_{\max}} \tilde{d}(a,t)\,D_V\big(c_b - c_0 e^{d/a}\big)4\pi a\,\mathrm{d}a\,. \quad (7)$$

Here $\tilde{d}(a,t)$ denotes a *void size distribution function* describing the fraction of voids with a specific size $a \in [a_{\text{vac}}, a_{\max}]$ at time t, *cf.*, Section 3. The source term $s(t)$ in Eq. (7) represents a *vacancy production rate* due to unbalanced diffusion which is caused by unbalanced diffusion in the sense of KIRKENDALL or by plastic deformation.

Once voids are nucleated diffusion is not the only mechanism which triggers their growth within the IMCs. To set up a general **variational model for void growth** we require the time-dependent constitutive equations to derive from rate potentials. Further we assume the power of the external forces acting on the material to be *completely* compensated by the rate potentials associated with void growth. Furthermore we imagine that the (initially very small) voids remain at every instance spherical and completely embedded in the material. Consider now one void surrounded by a sphere of material with radius b and let it expand for some reason. We neglect the elastic contribution to void growth and, thus, presume a *volume preserving deformation*. Then it holds for all $r \in [a,b]$, *cf.*, Figure 2:

$$\frac{\mathrm{d}}{\mathrm{d}t}\frac{4\pi}{3}(r^3 - a^3) = 0 \;\Rightarrow\; b = \big(b_0^3 - a_0^3 + a^3\big)^{\frac{1}{3}}\,, \quad (8)$$

where the index 0 refers to the initial state. The kinematic relation (8) will be employed subsequently to express functions of radius b as functions of current void radius a and the initial geometry. Furthermore, the rate of straining of the void surrounding material can be defined as

$$\dot{\epsilon} \overset{(\text{def})}{=} \frac{\partial \dot{r}}{\partial r} = \frac{\partial}{\partial r}\Big(\frac{a^2}{r^2}\dot{a}\Big) = \frac{2a^2}{r^3}\dot{a}\,. \quad (9)$$

The **external power** put into the system by an applied (positive or negative) pressure $p(t)$ is given by

$$\frac{\mathrm{d}}{\mathrm{d}t}\int_V p(t)\,dV$$

and for one void we obtain

$$P(\dot{a},a) = p(t)\,4\pi a^2\dot{a}. \quad (10)$$

In the solder material under consideration here the effect of thermal cycling is of particular interest. Therefore, temperature cycles $T(t)$ are considered to strain the material and to induce a pressure of the form

$$p(t) = \kappa^*(a)\;3\alpha\,[T_0 - T(t)] \quad (11)$$

where κ^* is the effective bulk modulus of the material and α is the thermal expansion coefficient. Following a classical approach of homogenization, *cf.*, [7], we obtain for an assemblage of spherical voids enclosed in an isotropic material with bulk modulus κ and shear modulus μ the effective bulk modulus κ^* as

$$\kappa^* = \kappa\left(1 - \frac{a^3}{b^3}\frac{3\kappa + 4\mu}{3\kappa + 4\mu b^3/a^3}\right). \quad (12)$$

The **rate of surface energy** of one void is written as

$$\Gamma(a,\dot{a}) = \frac{d}{dt}\big(4\pi a^2\gamma\big) = 8\pi a\gamma\dot{a}\,, \quad (13)$$

where γ is the surface energy per unit area [N/m].

The **creep-rate potential** is derived to account for the deformation of the material in which the void is embedded. Experimental observations reported in [1] indicate that the material near a void is subjected to a stress state that causes power-law creep, *i.e.*,

$$\dot{\epsilon} = \Big(\frac{\sigma_y}{\sigma_0(T)}\Big)^m \dot{\epsilon_c}\exp(-Q_c/RT)\,, \quad (14)$$

where $\dot{\epsilon}$ and σ are is the strain rate and the effective stress, respectively, σ_0 is the yield stress, m is a creep exponent and $\dot{\epsilon_c}$ is a material constance. The temperature dependence of the strain rate is controlled by the thermal activation energy Q_c. We summarize the last terms in Eq. (14) to a *reference strain rate*, $\dot{\epsilon}_{\text{ref}} = \dot{\epsilon_c}\exp(-Q_c/RT)$, with small values of $\dot{\epsilon}_{\text{ref}}$ corresponding to creep dominated deformation and $\dot{\epsilon}_{\text{ref}} \to \infty$ to a time independent behavior. The creep-rate potential per unit volume is given by

$$\int_0^{\dot{\epsilon}} \sigma_y\,\mathrm{d}\,\bar{\dot{\epsilon}} = \frac{m\sigma_0\dot{\epsilon}}{m+1}\left[\left(\frac{\dot{\epsilon}}{\dot{\epsilon}_{\text{ref}}} + 1\right)^{\frac{m+1}{m}} - 1\right]. \quad (15)$$

For simplicity we assume here a linear rate dependence, $m = 1$. By integration over the volume and with Eq. (9) the creep-rate potential for one void follows as

$$\Psi(\dot{a},a) = \int_a^b \frac{\sigma_0}{2\dot{\epsilon}_{\text{ref}}}\left(\frac{2a^2|\dot{a}|}{r^3}\right)^2 4\pi r^2\,\mathrm{d}r \quad (16)$$
$$= \frac{2\sigma_0}{\dot{\epsilon}_{\text{ref}}}\frac{4\pi a^3}{3}\Big|\frac{\dot{a}}{a}\Big|^2\left(1 - \frac{a^3}{a^3 + b_0^3 - a_0^3}\right).$$

The **diffusion rate potential** is derived from Eq. (6) as

$$\Phi(\dot{a},a) = \frac{E_V\dot{a}^2}{2D_V} - \frac{E_V\dot{a}}{a}\big(c_b - c_0 e^{d/a}\big). \quad (17)$$

With all details at hand we can now formulate an action integral $\mathcal{I}(\dot{a})$ as sum of all rate of energy contributions associated with the growth of voids. HAMILTON's principle simply requires stationarity of the action integral, $\delta\mathcal{I}(\dot{a}) = 0$, or, equivalently,

$$\frac{\delta}{\delta\dot{a}}\big(-P + \Gamma + \Psi + \Phi\big) = 0. \tag{18}$$

This ansatz yields an *ordinary differential equation* for void size $a(t)$,

$$\begin{aligned} 0 = &- 4\pi p(t)a^2 \; + 8\pi a\gamma \; + \frac{16\sigma_0\pi}{3\dot{\epsilon}_{\text{ref}}} a\dot{a}\Big(1 - \frac{a^3}{b^3}\Big) \\ &+ \; \frac{E_V\dot{a}}{D_V} - \frac{E_V}{a}(c_b - c_a)\,, \end{aligned} \tag{19}$$

which can be solved (numerically) for all different void sizes of interest.

3. Numerical simulations of void ensembles

The available material parameter for IMCs vary considerably. With typical values (from literature, *c.f.*, [3,6,8] and references therein and own measurements, no temperature dependence assumed) summarized in Table 1 and 2 we obtain for void condensation and growth the results outlined subsequently. The ODEs (19) have been solved numerically using the Matlab® solver `ODE45`.

Table 1
Material constants for diffusion

D_V [m^2/s]	c_0	c_b	d [m]	s [1/s]	γ [N/m]
10^{-17}	10^{-6}	10^{-4}	$5 \cdot 10^{-6}$	10^{-7}	1

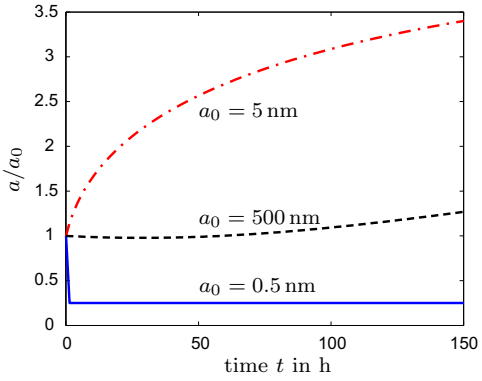

Fig. 3. Condensation of voids with different initial radii a_0 driven diffusion and surface energy contributions.

The beginning of void growth is the condensation of pores out of vacancy sized defects. It can easily be seen from Eq. (19) that for very small values of a_0 the last diffusion term dominates. If we initially neglect the external loading the void condensation process is driven by an interplay of vacancy diffusion and surface energy contributions. In particular, for the condition $c_b > c_a$ to be satisfied the initial size of the defect must exceed a critical nucleation radius which is here approximately 2-3 times the vacancy size, see Eqs. (2)-(4). Results for diffusion dominated void growth with different initial radii a_0 are displayed in Figure 3. Small defects with an initial radius of $a_0 = 0.5$ nm (twice the size of a vacancy in copper) collapse immediately. Defects of size greater than nucleation size will grow with a rate of void growth depending on the vacancy production rate. On the other hand, big voids, *e.g.*, $a_0 = 500\,\text{nm}$, basically fail to grow, here the effect of diffusion is too small for significant void growth within the time considered.

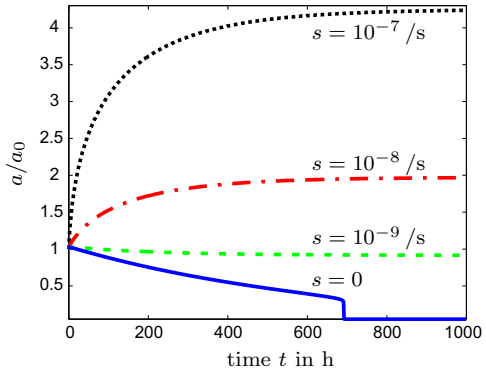

Fig. 4. Influence of vacancy production rate $s(t)$ on the condensation of voids driven by diffusion and surface energy contributions.

To keep voids growing a vacancy production source is required, otherwise the voids either collapse or reach a steady state — depending on the magnitude of surface tension. In the material under consideration the vacancy production results from the unbalanced diffusion, *i.e.*, the different diffusion coefficients of the migrating substances, [2]. In a first approximation its rate is assumed to be proportional to the ratio of the diffusion coefficients:

$$s(t) = \frac{c_K(t)}{t_{\text{ref}}}\frac{D_{\text{Cu}}}{D_{\text{Sn}}}\,, \tag{20}$$

where D_{Cu} and D_{Sn} are the diffusion coefficients of copper into tin and vice versa, t_{ref} is the total process time and c_K is a weighting factor which accounts for progressive IMC growth. Note that plastic deformation is an additional source of vacancy production and the factor c_K may also depend on the effective plastic straining. The influence of a given vacancy

production rate on void growth is illustrated by Figure 4 for voids of initial size $a_0 = 5$ nm.

To study the void growth for medium sized and big voids we subject the material to an external power resulting from temperature cycles between $-40°$C and 125°C within one hour, with 15 minutes dwell time at high and low peak temperature, respectively. Note that the external pressure computed from Eq. (11) must be understand as an *upper bound* of the real pressure acting in the solder as a consequence of thermal cycling of the whole microelectronic unit.

The evolution history of the voids strongly depends on the initial void size. Smaller voids clearly grow slower than then initially large ones. Comparing different void sizes in the same loading regime we find, e.g., within 500 min $a/a_0 \approx 1.5$ for $a_0 = 50\,\mathrm{nm}$ and $a/a_0 \approx 10$ for $a_0 = 500\,\mathrm{nm}$. That supports the experimental observation of few (relatively) large KIRKENDALL voids in IMCs.

Table 2
Elastic-plastic material constants

E [GPa]	κ [GPa]	μ [GPa]	σ_0 [MPa]	α [1/K]
100	80	50	450	$19 \cdot 10^{-6}$

Figure 5 displays void size *vs.* time for different reference strain rates. Small values of $\dot{\epsilon}_{\mathrm{ref}}$ clearly damp the evolution of voids. However, after enough time has passed the final void size will reach the same value as in the time-independent case. This final void size is determined by the external loading. Reference strain rates of $\dot{\epsilon}_{\mathrm{ref}} > 10^{-3}$ reflect a time-independent material behavior. This is in correspondence with experimental observations of creep in IMCs which has typical strain rates of $\dot{\epsilon}_{\mathrm{ref}} = 10^{-5} \ldots 10^{-4}/\mathrm{s}$.

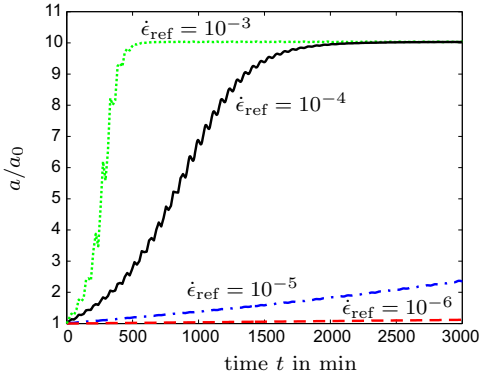

Fig. 5. Effect of creep on the growth of voids of initial size $a_0 = 500$nm for different reference strain rates within 50 temperature cycles.

4. Evolution of a void ensemble

In order to investigate an ensemble of voids with *different* initial radii we introduce – as already indicated in Section 2 – a void size distribution function $\tilde{d}(a, x, t)$. To derive an evolution equation for the void distribution we make use of a mesoscopic concept described in detail, *e.g.*, in [9,11]. Here we do not account for a dependence of the void distribution on the spacial position x, and put $\tilde{d}(a, x, t) = \tilde{d}(a, t) \equiv \tilde{d}$ and $\mathrm{d}\tilde{d}/\mathrm{d}x = 0$. Then we establish a balance equation for the void size distribution $\tilde{d}$ in the following form:

$$\frac{\partial \tilde{d}}{\partial t} + + \frac{\partial}{\partial a}\left[\tilde{d}\,\dot{a}(a)\right] = \Pi_V \ , \qquad (21)$$

where the production term Π_V summarizes the total and the mesocopic void sources, *cf.*, [12]. The value of $\dot{a}(a)$ can be calculated for given initial radii a_0 from Eq. (19).

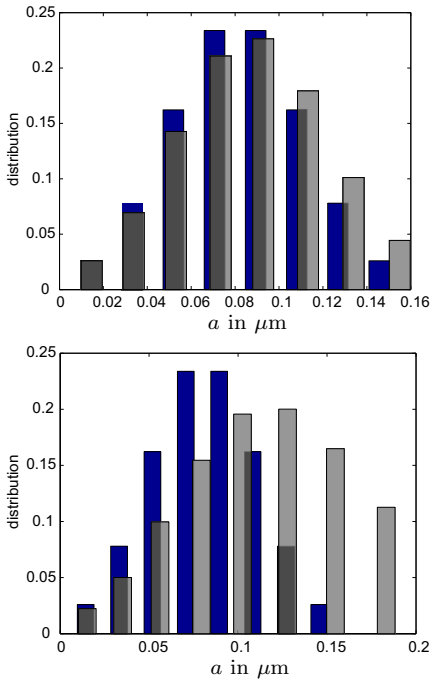

Fig. 6. Development of an initial GAUSSian void distribution after 1, 3 and 5 thermal cycles.

We start with a discretized GAUSSian distribution of 15 different void radii, $a = 10 \ldots 150$ nm. For a better understanding of the results we neglect any void production, *i.e.*, $s(t) \doteq 0$ in Eq. (7). Within several steps of thermal cycling we obtain the temporal development of $\tilde{d}$ as illustrated in Figure 6. The initially symmetric distribution changes to an

asymmetrical distribution in such a way that the fraction of smaller voids decreases and the bigger voids grow. Such results correspond to the well established LSW-theories for OSTWALD ripening, [10], where bigger "grains" grow at the expense of the smaller ones. In the vacancy diffusion dominated first stages of our model the GIBBS-THOMSON effect has a similar result void growth. Then, during proceeded growth the voids reach a size, for which their growth is characterized primarily by plastic deformation. (To reduce the computational time the reference strain rate is set to $\dot{\epsilon}_{\text{ref}} = 1$ in this section which corresponds to an immediate plastic response). In the long time behavior the size distribution function differs considerably from a typical LSW distribution. In particular the fraction of large voids extremely exceeds the fraction of small voids.

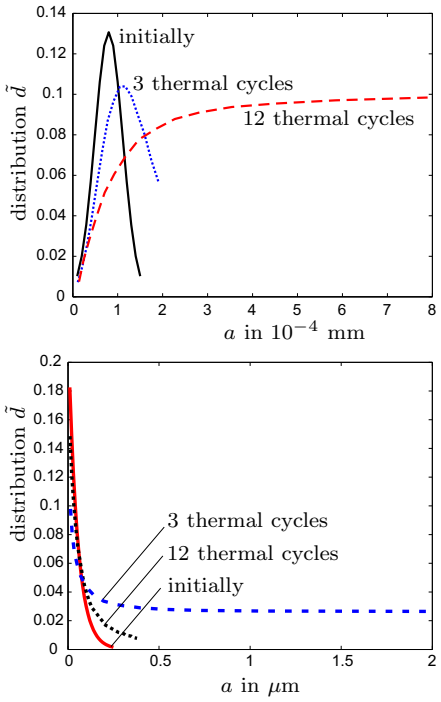

Fig. 7. Evolution of void distribution $\tilde{d}$ in the long range, *1st row*: initially Gaussian distribution. *2nd row*: initially exponential distribution.

Figure 7 shows a different view on the evolution of $\tilde{d}$ and it can be seen how the final void size distribution differs from the initial GAUSSian form (*1st row*). Moreover, in an attempt to model a more realistic initial distribution with a dominance of small voids in the initial state Figure 7 (*2nd row*) displays the evolution of $\tilde{d}$ starting from an exponential distribution of 25 voids within $a = 10 \ldots 250$ nm. Again we observe a growth of the big voids at the cost of the smaller ones. In particular, the void size a reaches large values and the distribution function is stretched over a wide range of void sizes. The simulations has been stopped after a void volume fraction of $\approx \frac{2}{3}$ was reached since our model does not account for damage due to void coalescence. Unfortunately this limits the predictive capabilities of the void size distribution analysis. However, already a significant amount of large voids in a material clearly indicates the onset of failure.

The presented results are applicable to derive the temporal evolution of the effective properties of voided materials. The constitutive model shall be incorporated on the material point level in FEA tools to study the mechanical behavior of IMCs under realistic loading regimes. Such analyzes then allow for a systematic prediction of live time and strength of joining connections in MEMS.

Acknowledgment

The authors gratefully acknowledge the support of the German Federal Environmental Foundation (DBU).

References

[1] A. F. Bower and L. B. Freund. *J. Appl. Phys.* 74: 3855-3868,1993.
[2] J.W. Cahn and J.E. Hilliard. *Acta Metall. Mater.*, 19:151–161, 1971.
[3] B. Chao, S.H. Chae, X. Zhang, K.H. Lu, J. Im, and P.S. Ho. *Acta Mater.*, 55(8):2805–2814, 2007.
[4] A. Cuitino and M. Ortiz. *Acta Metall. Mater.*, 44:427–436, 1995.
[5] F.D. Fischer and J. Svoboda. Void growth due to vacancy supersaturation — a non-equilibrium thermodynamics study. to appear in *Scripta Mater.*, 2007.
[6] G. Galyon. *IEEE T. Electron. Pack.*, 28(1):94–122, 2005.
[7] K. J. Lee and R. A. Westerman. *J. Composite Mat.*, 4:242–252, 1970.
[8] Z. Mei, M. Ahmad, M. Hu, and G. Ramakrishna. *Proceedings 55th Electronic Components and Technology Conference*, Orlando, USA, 2005 (IEEE), pp. 415-420
[9] C. Papenfuss and P. Ván and W. Muschik. *Arch. Mech.*, 55(5-6):459-477, 2003.
[10] C. Wagner. *Z. Elektrochem.*, 65(7-8):581–591, 1961.
[11] K. Weinberg and T. Böhme. Mesoscopic Modeling for Continua with Pores: Biological Soft Tissue. *to appear in: J. Non-Equil. Thermody.*, 2008.
[12] K. Weinberg and T. Böhme. Mesoscopic Modeling for Continua with Pores: Dynamic Void Growth in Visco-Plastic Metals. *to appear in: J. Non-Equil. Thermody.*, 2008.